FOCUS REVIEW

π-Conjugated polymer nanowires: advances and perspectives toward effective commercial implementation

Wesley K. Tatum[1] · Christine K. Luscombe[1,2,3]

Abstract

π-Conjugated polymers have continued to demonstrate their relevance and ability to be used in next-generation electronic and optoelectronic devices. Nanowires formed from semiconducting polymers can be easily produced and aligned, which considerably enhances the polymer's properties, such as charge transport. This review discusses recent advances in the formation and alignment of semiconducting polymer nanowires. This includes whisker growth and self-assembly methods, as well as methods of nanoscopic confinement through composites and blends. Next, this review explores how semiconducting polymer nanowires have been successfully implemented in field-effect devices, sensors, and thermoelectrics.

Introduction

During the past few decades, π-conjugated polymers (CPs) have been developing toward full implementation in commercial devices. There has been immense progress toward understanding these materials, as well as their design, synthesis, and applications [1–8]. The promising properties of CPs can enable flexible, and perhaps even stretchable (Fig. 1) optoelectronic devices, which are produced through low-cost, high-throughput methods, such as roll-to roll (R2R) processing [9–12]. High-throughput or continuous production methods are important to develop because the strength of CP devices lies in their ability to be produced and processed at such scales relatively cheaply. However, despite the immense progress this field has seen, energetically cheap devices with high electronic efficiencies are yet to be realized. This is largely due to the fact that quantitative structure–property relationships are difficult to determine in CPs as a result of their semicrystalline or highly amorphous nature [13–16]. The morphology and crystallinity of thin films made from CPs are highly influenced by the chemical structure and molecular weight of the polymer, the choice of solvent, annealing conditions, and many other variables throughout the thin-film production [9, 17–22]. Highly variable morphology is problematic because the properties and performance of a CP device are highly dependent on the morphology of the CP active layer.

To address the problems arising from inconsistent and largely unpredictable morphologies of CP thin films, nanowires have been extensively used to produce highly crystalline CP active layers. CP nanowires can be produced in a number of ways, each of which results in an increase in the charge transport and crystallinity as well as a decrease in the bandgap, relative to the bulk CP material [23, 24]. This effect can be amplified by aligning groups of nanowires along a given axis because nanowires exhibit anisotropic light interactions and charge transport. Alignment of the nanowires exploits this anisotropy by ensuring electrical currents or chemical gradients will occur specifically along axes of the nanowires that have improved properties [25, 26]. CP nanowires offer the opportunity to reduce the size of devices while maintaining or increasing performance, stability, and mechanical properties [23, 27–33].

✉ Christine K. Luscombe
luscombe@uw.edu

1 Department of Materials Science and Engineering, University of Washington, Seattle, WA 98195-2120, USA

2 Department of Molecular Engineering and Sciences, University of Washington, Seattle, WA 98195-1652, USA

3 Department of Chemistry, University of Washington, Seattle, WA 98195-1700, USA
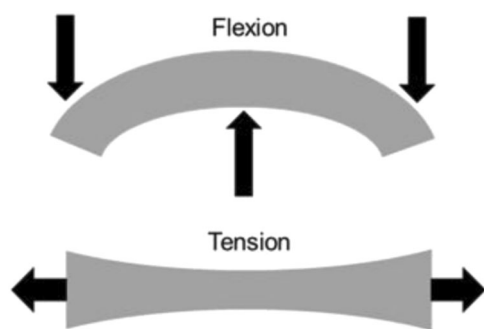
Fig. 1 A graphical description of stretching and flexing for thin films. Reprinted with permission from ref. [12]

This focus review is divided into two main parts. The first will explore recent advances and developments in the formation and alignment of CP nanowires. Broadly, this will include methods of self-assembly and nanoscopic confinement. After that, there will be a discussion of different device applications of CP nanowires where we will focus largely on organic field-effect transistors (OFETs), sensors, and thermoelectrics. For a discussion of other important CP devices, such as organic photovoltaics (OPVs), readers are directed to other review articles [33–37].

Approaches to formation and alignment

Self-assembly of nanowires

Perhaps the easiest and most common method of nanowire formation is through the "whisker" method. In this method, a poor solvent for the CP is used. The CP/solvent mixture is heated and stirred to ensure complete dissolution of the CP and, as the solution cools undisturbed, the polymer chains readily self-assemble into nanowires that are typically 15–20 nm wide, 5 nm tall, and up to several microns in length. The specific dimensions and properties of the nanowires are determined by the side-chain length, solvent choice, and solvent temperature [38–40]. The time that the solution is left to self-assemble, referred to as aging, is an effective lever for controlling the crystallinity and, therefore, electronic properties of the nanowires. The resulting solutions of nanowires can be cast into devices as is. A representative atomic force microscopy micrograph of spin-cast poly(3-hexylthiophene) (P3HT) nanowires is seen in Fig. 2. For example, aging of the solution can induce increases in charge mobility by as much as three orders of magnitude parallel to the direction of alignment [41]. This is attributed to improving long-range order and increases in intermolecular interactions, or H-type aggregation as described by the Spano model [24]. Such high degrees of
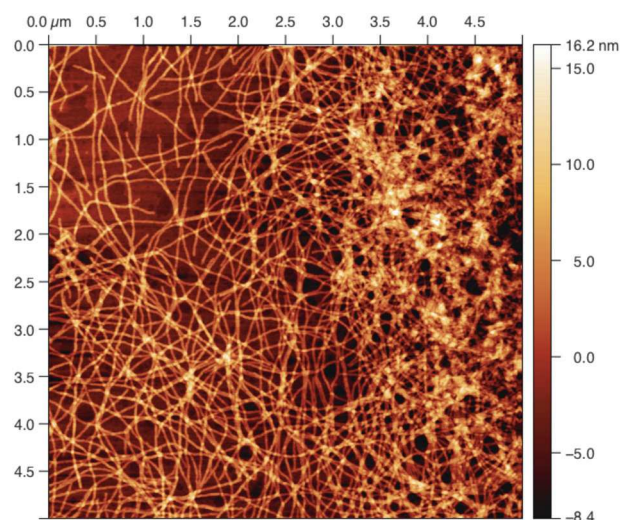

Fig. 2 AFM micrograph of P3HT nanowires

long-range order are particularly attractive for device applications, such as OFET, where charge transport through the CP is crucial.

In addition to aging, it is common to seed nanowire growth to quickly produce nanowires with even higher crystallinity. Rather than relying on amorphous aggregates to initiate crystallization, seeded growth builds from a highly crystalline aggregate, which helps coordinate growth through the nanowire. There are two main methods to produce seeds for growth of CP nanowires—sonication and exposure to ultraviolet (UV) light [21, 40, 42–46]. It has been shown that by dissolving P3HT into a mixture of non-polar, good solvent (e.g., chlorobenzene) and some polar, poor solvent (e.g., acetonitrile), aggregates of P3HT chains begin to assemble. Short, intense cycles of sonication separate the highly disordered aggregates and allow them to form highly ordered crystals, which can then rapidly grow into highly crystalline nanowires [47]. Alternatively, it has been shown that brief exposure to UV light can induce similar aggregations. UV light is well-known as a source of decomposition in CP, however short exposure can energetically activate CP into a quinoid-like structure and promote the π–π interactions between the polymer chains that drive crystallization [43]. These UV-induced aggregates also serve as highly ordered nucleation centers for CP nanowires. For a rigorous investigation into the effects of UV- and sonication-induced crystallization as well as casting methods and their effects on charge mobility, readers are directed to the following articles [48, 49].

Aged nanowires are typically produced in batches and then cast into films. This method is acceptable for laboratory-scale experiments; however, it is insufficient for any industrial-scale implementation of CP nanowires due to the slow and variable nature of batch production.

Continuous production methods need to be explored for CP nanowires to be considered for commercial implementation. One such method utilizes microfluidic techniques and laminar flow to seed, age, and align CP nanowires for casting into thin films and is shown below in Fig. 3a. The trial polymer, P3HT, was dissolved into chloroform and, using a combination of controlled cooling and exposure to UV light (or sonication), the solution was seeded into nanowire growth [48, 49]. Simply tuning the flow rate of the system allows for precise control of the nanowire aging. A combination of continuous flow nanowire formation and blade casting has demonstrated films with an unprecedented degree of alignment, over 80%, rather than the stochastic distribution of alignments that is produced during spin-casting. This high degree of alignment is highlighted in Fig. 3b. In this method, there are molecular connections between the aligned nanowires that increase and secure nanowire orientation. It is believed that these physical connections are either tie chains or a result of the "shish-kebab"-type nucleation, with these interactions driving the strong alignment tendencies. As such, OFETs made from these highly aligned films have hole mobilities of 0.16 cm^2/V s, more than an order of magnitude greater than those of the P3HT thin films (0.013 cm^2/V s) [50].

Nanowire alignment

There are many methods by which CP nanowires can be aligned in a thin film, each of which can produce highly ordered and aligned films of nanowires. For example, excellent morphology and mobility has been produced by drop casting CP solutions onto an angled substrate [51], or directing nanowire growth via an external bias [52]. Such methods are novel and useful for laboratory-scale research into the properties of CP films and crystallites. However, these methods are not readily scalable to the level required by continuous production methods like R2R printing.

Blade printing is a unique method for continuously creating thin films. The shearing force between the print head and the substrate has been shown to induce a degree of alignment parallel to the direction of motion [53, 54]. By adjusting the geometry of the blade, this alignment can be greatly increased and, in combination with UV light exposure, aligned nanowires can be formed, as depicted in Fig. 4a [49, 55]. Adjusting the blade geometry (Fig. 4b–g) and printing speed, with UV-seeded nanowires, can increase the average mobility of OFET devices by an order of magnitude from 0.0013 to 0.013 cm^2/V s. These easily controlled and modified processing conditions can be used
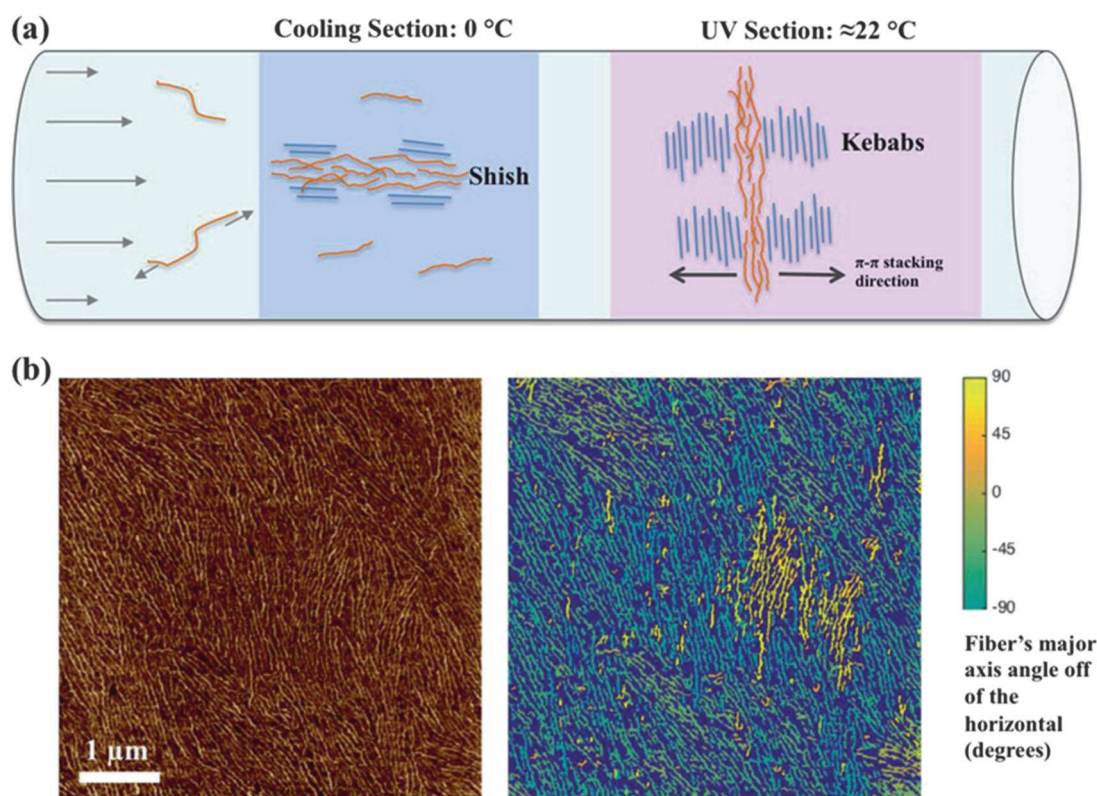

Fig. 3 a Proposed mechanisms of nucleation and growth in the flow-cooling UV system. In the cooling section, solution instability and shear force cause the formation of shish nuclei. The π–π stacks align with the flow as they grow longer in the UV section. **b** Left: 5 µm × 5 µm AFM image of the surface of the MCU-0.25 device. Right: same image, segmented for the identification of P3HT nanofibers and their angles off of the horizontal. Reprinted with permission from ref. [50]

Fig. 4 a Scheme of the BPD-UV fabrication concept; the SEM images of the BPD-UV fabrication blade: **b** parallel; **d** prismatic; **f** wave-like features; and corresponding conjugated polymer films (**c, e, g**) in the same printing conditions (tapping mode AFM phase images (5×5 μm and 2×2 μm)). All the scale bars in the SEM images are 40 μm. Reprinted with permission from ref. [55]
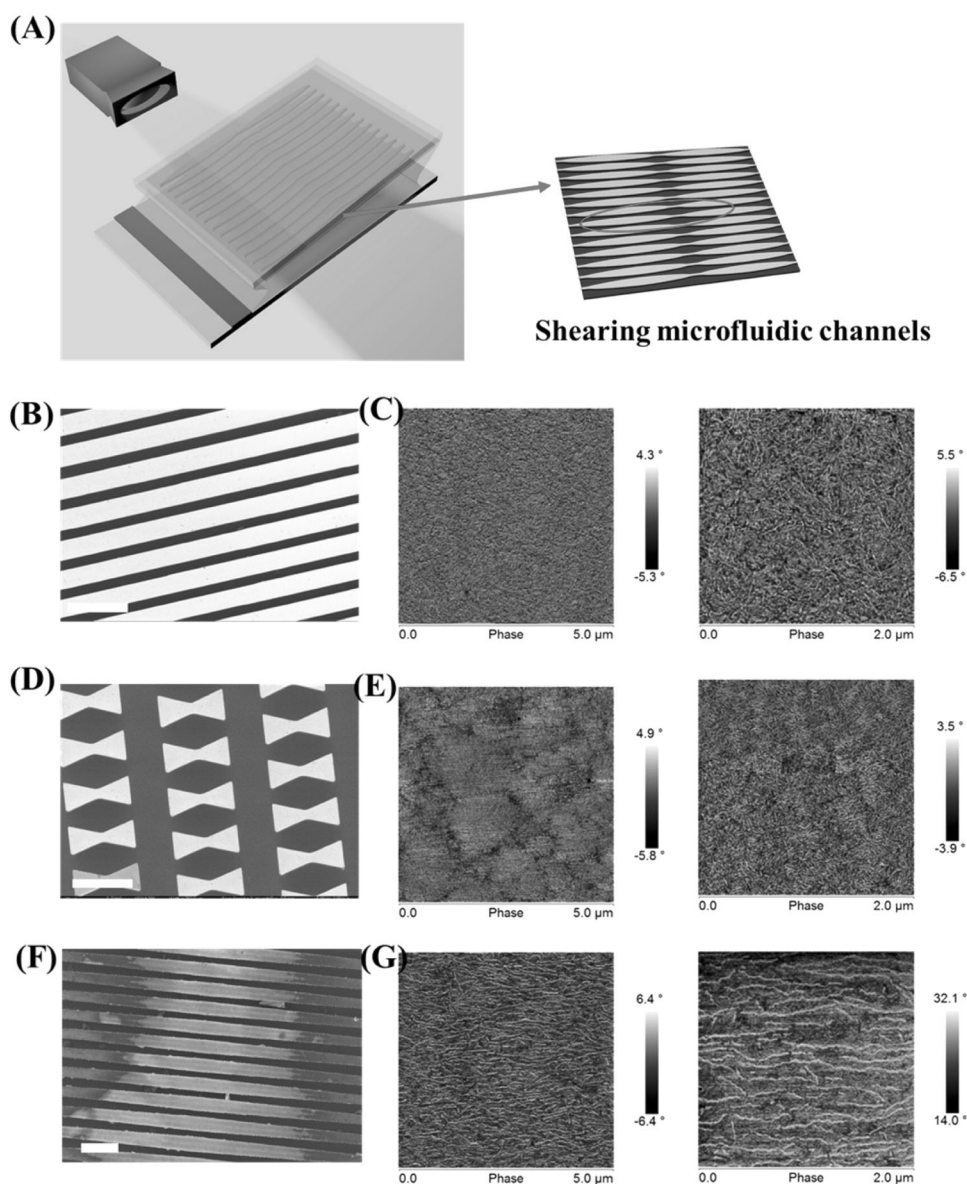
to effectively tune the degree of aggregation and crystallinity. The ability of the print head to influence the morphology of films is unique and requires further exploration, especially in combination with other aforementioned techniques. For instance, blade printing of the solutions of UV-seeded, microfluidically grown nanowires could increase the crystallinity of the films or help direct the aggregation of blends of nanowires in elastomers. These techniques can be used on their own or in combination, depending on the CP system, to continuously produce highly ordered nanowire films.

Nanoscopic confinement

Networks of nanowires have been shown to retain their high bulk charge mobility, even within insulating host matrices

and at low volume fractions [56–59]. By utilizing the intrinsic flexibility of CP and the stretchability of an elastomeric matrix, stretchable and robust electronic devices have been produced by different groups. Intrinsic stretchability is important to note because electronic devices that function despite mechanical elongation and duress are key to wearable and body-integrated electronics and has, to the best of our knowledge, yet to be fully demonstrated as highly scalable and continuously producible by inorganic or hybrid semiconducting materials [60]. Solutions of CP nanowires can be blended with elastomers such as poly (dimethylsiloxane) (PDMS) to create OFET semiconducting layers with increased hole mobilities and fatigue resistance. A P3HT nanowire solution was mixed at a ratio of 1:3 with PDMS, resulting in a mobility of $\mu = 0.11$ cm^2/V s, which is over double that of the pure
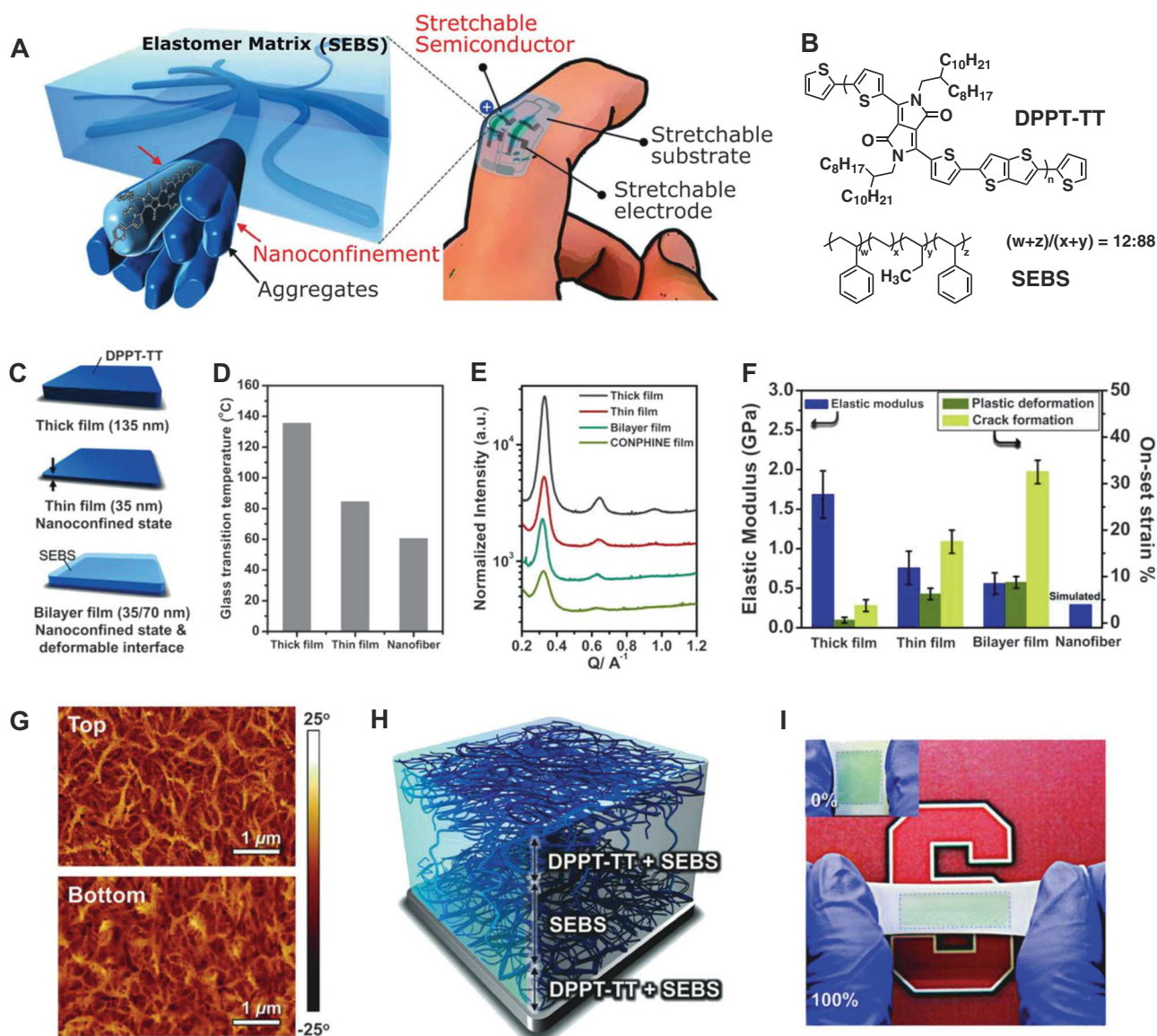
Fig. 5 Nanoconfinement effect for enhancing the stretchability of polymer semiconducting film through the CONPHINE method. **a** A 3D schematic of the desired morphology composed of embedded nanoscale networks of polymer semiconductor to achieve high stretchability, which can be used to construct a highly stretchable and wearable TFT. **b** Chemical structures of semiconducting polymer DPPT-TT (labeled as **1**) and SEBS elastomer. **c** Three model films of DPPT-TT for investigation of the nanoconfinement effect (i.e., increased chain dynamics and suppressed crystallization). **d** Glass transition temperatures of the thick, thin, and nanofiber films. **e** XRD line cuts for three model films and the CONPHINE-**1** with 70% SEBS film along the q_{xy} axes, normalized by the exposure time and volume of DPPT-TT layer and offset for clarity. **f** Elastic moduli, onset strains of plasticity, and onset strains of crack of the model films, with the simulated modulus of the nanofiber film. The error bars of elastic moduli and onset strains represent the standard deviation and the range of measurement error, respectively. **g** AFM phase images of the top and bottom interfaces of the CONPHINE-**1** film with 70 wt% SEBS. **h** A 3D illustration of the morphology of the CONPHINE-**1** film. **i** Photographs of a CONPHINE-**1** film (blue area) at 0% strain and stretched to 100% strain on a rubber substrate. Reprinted with permission of ref. [63]

P3HT nanowire reference film [61]. In addition to higher mobilities, the blend film showed no significant fractures or cracks after elongation of 100%. This is consistent with films of poly(3-butylthiophene) (P3BT) nanowires that were blended with poly(styrene) (PS). In this case, a film consisting of P3BT nanowires present in volume percentages as low as only 2% in PS demonstrated a $\mu = 0.014\ \mathrm{cm^2/V\ s}$, as compared to the 100% P3BT film, which demonstrated $\mu = 0.0089\ \mathrm{cm^2/V\ s}$. The mixture with the highest mobility contained 17.5 vol% P3BT nanowires at $\mu = 0.016\ \mathrm{cm^2/V\ s}$ [62]. Rather unexpectedly, it is common for blends of CP nanowires in insulating matrix to demonstrate higher mobilities than their neat counterparts. This is attributed to increased molecular order in the

nanowires of the blend films. This increased order in the CP arises from the incompatibility between the nanowires and the host matrix, which drives the nanowires to reduce their interactions with the elastomer. Notably, this led to a vertical phase separation between P3HT nanowires and PDMS, with the nanowires preferring to form highly interconnected networks at the substrate interface and the PDMS preferring the air interface. We would like to point to this as a facile route for increasing encapsulation of air sensitive CP nanowires, while drastically improving mechanical robustness.

As opposed to allowing CP molecules to self-assemble on their own and then blending them, it has been shown that confining the CP in an incompatible matrix is an effective method for forming nanowires. In this technique, a host material forces the CP to aggregate and assemble into nanowires (Fig. 5a, g, h) [63]. In both composites and copolymers, the confining moiety is typically an insulating material with elastomeric properties. By mixing the two together, it is possible to retain the mechanical properties of the host matrix, while still displaying many of the optoelectronic properties of the CP fraction, as shown in Fig. 5d–f, i. For instance, the recently developed CONPHINE method, Fig. 5, involves mixing low weight percentages of CP, in this case poly(2,5-bis(2-octyldodecyl)-3,6-di(thiophen-2-yl)diketopyrrolo[3,4-c]pyrrole-1,4-dione-alt-thieno[3,2-b]thiophen) (DPPT-TT), with PS-co-(ethylene-b-styrene)) (SEBS), shown in Fig. 5b. These mixtures can be used to make highly stretchable OFET devices with mobilities of up to $\mu = 1.32$ cm^2/V s while being stretched to 100% elongation for 100 cycles. This is in stark contrast to the reference pristine DPPT-TT films, whose mobility dropped over three orders of magnitude after 100 cycles of elongation to 100% [63]. Despite having such a large weight fraction of insulating polymer in CP: elastomer blends and composites, the low percolation threshold of CP nanowire networks allows for charges to flow freely, yielding a highly stretchable OFET, which retain their performance during stretching, twisting, and quite notably, poking [60–63]. This is highly desirable in devices that conform to skin or highly mobile joints, where many varied deformations will repeatedly occur during device operation.

Device applications

Field-effect devices

The unique properties of CP nanowires make them particularly well-suited for implementation in field-effect devices. As has been explored in the above sections, low percolation thresholds and increased charge transport properties allow for highly performing OFET devices made from aligned nanowire films or blends of nanowires with insulating materials. Beyond this, the high aspect ratio of CP nanowires allows for OFETs to be made from single nanowires, which have exhibited charge mobilities and on/off ratios as much as two orders of magnitude higher than pristine thin-film counterparts [64]. Single-nanowire devices are particularly exciting due to their reduced device dimensions, which allows for more devices to occupy a given area. So, using CP nanowires, rather than thin films, increases device density while simultaneously increasing device performances. For instance, single-nanowire devices made from two different diketopyrrolo-pyrrole polymers demonstrated a full order of magnitude increase in both mobility and on/off ratio over the thin-film analogs [65]. The single-nanowire OFET mobilities for PDPP2TBDT were $\mu_h = 7.42$ cm^2/V s and $\mu_e = 0.04$ cm^2/V s showing a high hole mobility and moderate electron mobility. PDPP2TzBDT displayed high mobilities for both holes and electrons, $\mu_h = 5.47$ cm^2/V s and $\mu_e = 5.33$ cm^2/V s, which is among the highest mobilities reported among ambipolar OFETs to date [65]. Not only has it been confirmed that charge transport properties are enhanced through implementation of CP nanowires over thin films, it has been shown that there is a significant reduction in the low-frequency spectral noise of the resulting devices [66]. Noise in electronic devices is a distortion of the signals that flow through them, making it difficult to distinguish between modes of operation. This is particularly prevalent at low voltages and currents where the signal-to-noise ratio is low. In order to make low-energy-consumption devices, like body-integrated sensors, devices need to be able to function at lower voltage and current values, making noise a prevalent problem. One type of noise scales as $1/f$, where f is the frequency of the signal, and is described by the Hooge parameter, which is defined for homogeneous samples as

$$\frac{S_I}{I^2} = \frac{\alpha_H}{Nf}$$

where S_I is the spectral density of the current, I is the current, N is the number for free charge carriers, and α_H is the Hooge parameter. Compared to thin-film devices, nanowire devices consistently exhibited an order of magnitude reduction in α_H. This confirms that α_H noise in OFET devices is related to the structural coherence of the semiconducting layer [66]. By using highly ordered nanowires, as opposed to thin films, noise in devices can be suppressed. All of these results indicate that many major device performance metrics of field-effect devices can be greatly improved through the use of nanowires over thin films. Additionally, the use of single-nanowire devices can

greatly decrease the dimensions of devices without sacrificing performance. This reduction in device size can be used to develop high-performance, flexible computers, which are particularly pertinent to body-integrated devices, where the computer footprint and flexibility are critical.

Sensing devices

The bulk of the research into sensing materials is focused on inorganic materials and graphene derivatives (e.g., single- or multi-wall carbon nanotubes), but CPs and CP nanowires offer unique solutions for large-scale production, while still maintaining high responsivity and producing robust devices. In fact, recently published CP-based devices perform comparably to inorganic and graphene-based devices [31, 33]. Additionally, CP-based devices can have significant tunability in their response ranges, as small changes in the polymer backbone can precisely modulate electronic and chemical properties. These changes can also be used to functionalize CPs to interact with and respond to specific chemical and biochemical analytes [67–77]. When used in sensing devices, CPs exhibit massive changes in their properties as a response to specific external stimuli, such as light, pressure, and chemical environment, making CP nanowires exceptionally promising candidates.

In ammonia sensing, a response arises due to charge carrier traps created as the ammonia molecules adsorb onto the surface of the nanowires. The higher crystallinity of CP nanowires compared to CP thin films means that any externally induced defects will more significantly affect the charge mobility of the material. On top of this, the high surface-to-volume ratio and higher intrinsic mobilities of CP nanowires compared to CP thin films increases the sensitivity and signal-to-noise ratio, respectively. By creating OFETs from P3HT nanowires, it was shown that real-time sensing of ammonia from 25 ppm down to a limit of detection (LOD) of 8 ppb is possible, producing the highest sensitivity in real-time ammonia sensors at the time of publishing [31]. This is compared to thin films of P3HT, which were only a third as sensitive to changes in ammonia concentration, as shown in Fig. 6. So, chemicals that can interact and adsorb onto the surface of a CP can be sensed more effectively by nanowires, rather than thin films. This change in mobility has been exploited to detect a wide variety of compounds, such as water [78], peroxides [79], and heavy-metal ions [80].

In addition to high sensitivities to chemicals, CP nanowires are also highly sensitive to light. This sensitivity has been exploited to devise phototransistors, photodetectors, and photodiodes [81–86]. There is great interest in producing high-sensitivity, low-noise optical sensing devices that are flexible and cheap to produce, especially those sensitive to either white light or infrared and near-infrared (NIR) light (for use in thermal imaging). One compelling example of the effectiveness of CP nanowires is in work done on poly(bis(2-oxoindolin-3-ylidene)-benzodifuran-dione-thienothiophene) (PBIBDF-TT), which is a low-bandgap donor–acceptor CP [87]. As a thin-film phototransistor, the photoresponsivity (R) and photo-current/dark-current ratio (P) were found through illumination with an NIR light source. $R_h = 60$ mA/W, $P_h = 10$, and $R_e = 20$ mA/W, $P_e = 6$ for p-type and n-type transport, respectively. These values were significantly improved by switching from thin film to nanowire active layers, with $R_h = 440$ mA/W, $P_h = 1.3 \times 10^4$, and $R_e = 70$ mA/W, $P_e = 3.3 \times 10^4$. Clearly, the sensitivity and response of phototransistors are greatly improved by the use of nanowires, instead of thin films.

Detecting changes in the mobility of CP nanowires is an excellent method for detecting the presence of an analyte, but it is not the only type of signal that can be used for sensing. Another method of signaling is through fluorescence, which is used in optical sensors. Optical sensors function by detecting the quenching of fluorescence in the CP as a response to the presence of an analyte. These decreases in fluorescence are easily and precisely

Fig. 6 (Left) Structure of a nanowire-based OFET ammonia sensor. (Right) A comparison between the responses and sensitivities of the nanowire-based sensor and the thin-film-based sensor. Reprinted with permission of ref. [31]
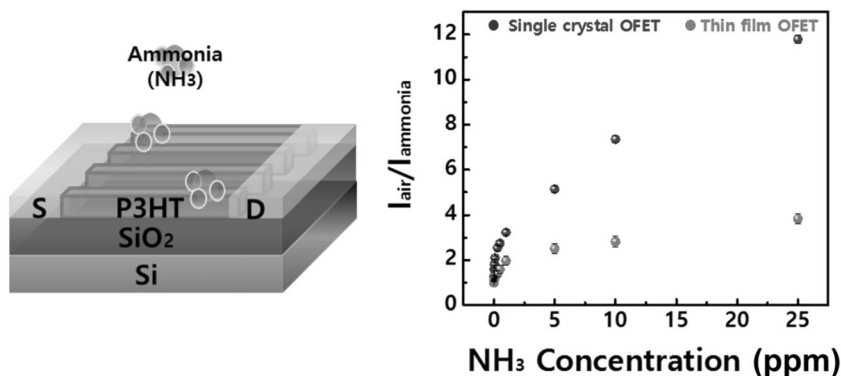
detectable, which make optical sensors highly sensitive [70–76, 88, 89]. Fabricating optical sensors from highly porous networks of CP nanowires can further improve the impressive properties of optical sensors by utilizing the high surface-to-volume ratios of nanowires and the large surface areas of porous structures to produce devices that show sensitivities two to three orders of magnitude higher than thin films of the same materials. Fluorescent CP nanowire networks have been successfully implemented in optical sensors with LOD in the parts per billion levels for Fe^{3+}, Hg^{2+}, and 2,4-dinitrotoluene while still maintaining response times of milliseconds [90]. CP nanowires are known to display excellent fluorescence and have been used in light-emitting applications, such as in OLEDs [91–94]. Optical sensors are a natural extension of this utility and have demonstrated a high capacity for performance. In order to begin the transition toward large-scale production of flexible chemical and optical sensors, functionalized CP nanowires should continue to be researched and their compatibility with the previously outlined methods for nanowire formation should be investigated.

Thermoelectric devices

Thermoelectric generators convert a difference in temperatures into electricity. In order for materials to successfully be used as active layers in thermoelectric generators, they must simultaneously possess high electronic conduction and low thermal conduction [95–98]. Inorganic materials typically dominate this field, but CPs have recently begun to be explored because of their intrinsically low thermal conductivity, solution processability, and flexibility, which enables low operation temperature, conformal devices that demonstrate similar thermal power conversion at room temperature as the typical inorganic devices (e.g., $BiTe_3$) [99]. Unlike field-effect devices, which use an electrical bias to dope the semiconducting active layer, thermoelectric devices require deliberate electrical or electrochemical doping to achieve a high concentration of free charge carriers [96, 98, 100, 101]. This doping requires the presence of counter-ions, which drastically alters the morphology of a thin film and thereby decreases the mobility of the charge carriers [97, 101, 102]. Experiments into the extent of the impact that morphology has on the power factor in CP has clearly shown that the more aligned and ordered crystalline domains are the higher the power factor is [101]. In order to decrease the effect that doping has on morphology, researchers have utilized CP nanowires, which have a higher degree of molecular order, mobility, and, in fibrous networks, amounts of void space that further decreases thermal conductivity [102]. The morphology is also more stable in CP nanowires due to their high surface-to-volume ratio and the fact that dopants cannot diffuse into the crystal

structure [103]. It has also been shown that CP nanowires tend to possess higher Seebeck coefficients than their thin-film counterparts, due to sharper features in their density of states near the Fermi level, further increasing their thermoelectric power factor [104]. In the case of P3HT, nanowire mats with large void fractions displayed higher figures of merit, ZT, than the thin-film alternative, with $ZT = 0.016$ and 0.0098, respectively. The higher figure of merit for the nanowire mat than the neat film was attributed to a higher intrinsic mobility and lower thermal conductivity. The thermal conductivities were $\kappa = 0.0708$ and 0.158 W/m K for the nanowire mat and thin film, respectively. Conversely, the thin film possessed higher power factor, $P = 5.2 \times 10^{-6}$, than the nanowire mat, $P = 3.7 \times 10^{-6}$. This is attributed to the thin film's higher overall doping, which increased the Seebeck coefficient to a greater extent [102]. This promising result is consistent with the more well-studied, conducting polymer poly(3,4-ethylenedioxythiophene) (PEDOT) nanowires, which demonstrated higher charge mobility, Seebeck coefficient, and lower thermal conductivity than the thin-film PEDOT [104]. This implies that high-mobility CP nanowire mats that are more fully doped could obtain extremely high power factors.

Conclusion: outlook and opportunities

As a field, CPs have demonstrated remarkable improvements and advances over the past decade. These have been catalyzed by an increased understanding of the effects of chemical structure modifications and the advent of high-mobility donor–acceptor polymers, as well as the improved processing of these materials. There are many promising opportunities for the commercial implementation of CPs as field-effect devices, sensors, thermoelectric devices, as well as OPVs and light-emitting devices. Their flexibility and ability to be scalably processed opens the door for their use as conformable, wearable, or body-integrated devices, and other flexible devices that are of high interest. The high tunability of their mechanical and electrical properties and their stimuli-responsive behavior enable CPs to be specifically designed and optimized for these different applications.

These strengths of CP materials are greatly enhanced by forming them into nanowires. Nanowires have greatly increased electrical and thermoelectric properties due to their higher level of molecular ordering and reduced number of defects compared to thin films. By implementing nanowires as an aligned film, as a composite with an elastomer, or as a mat, the mechanical properties of the nanowires can be tuned to survive elongations beyond 100%, increase specificity and response to analyte interactions, or further augment CP electronic properties.

Compliance with ethical standards

Conflict of interest The authors declare that they have no conflict of interest.

References

1. Bin H, Gao L, Zhang Z-G, Yang Y, Zhang Y, Zhang C, Chen S, Xue L, Yang C, Xiao M. et al. 11.4% Efficiency non-fullerene polymer solar cells with trialkylsilyl substituted 2D-conjugated polymer as donor. Nat Commun. 2016;7:13651

2. Zhou H, Yang L, You W. Rational design of high performance conjugated polymers for organic solar cells. Macromolecules. 2012;45:607–32.

3. Yue W, Nikolka M, Xiao M, Sadhanala A, Nielsen CB, White AJP, Chen H-Y, Onwubiko A, Sirringhaus H, McCulloch I. Azaisoindigo conjugated polymers for high performance N-type and ambipolar thin film transistor applications. J Mater Chem C. 2016;4:9704–10.

4. Morin P-O, Bura T, Leclerc M. Realizing the full potential of conjugated polymers: innovation in polymer synthesis. Mater Horiz. 2016;3:11–20.

5. Thomas SW, Joly GD, Swager TM. Chemical sensors based on amplifying fluorescent conjugated polymers. Chem Rev. 2007;107:1339–86.

6. Colladet K, Fourier S, Cleij TJ, Lutsen L, Gelan J, Vanderzande D, Nguyen LH, Neugebauer H, Sariciftci S, Aguirre A. et al. Low band gap donor−acceptor conjugated polymers toward organic solar cells applications. Macromolecules. 2007;40:65–72.

7. Tessler N, Denton GJ, Friend RH. Lasing from conjugated-polymer microcavities. Nature. 1996;382:695–7.

8. Facchetti A. π-Conjugated polymers for organic electronics and photovoltaic cell applications. Chem Mater. 2011;23:733–58.

9. Gu X, Zhou Y, Gu K, Kurosawa T, Guo Y, Li Y, Lin H, Schroeder BC, Yan H, Molina-Lopez F. et al. Roll-to-roll printed large-area all-polymer solar cells with 5% efficiency based on a low crystallinity conjugated polymer blend. Adv Energy Mater. 2017;7:1602742

10. Khim D, Ryu G-S, Park W-T, Kim H, Lee M, Noh Y-Y. Precisely controlled ultrathin conjugated polymer films for large area transparent transistors and highly sensitive chemical sensors. Adv Mater. 2016;28:2752–9.

11. Kim T, Kim J-H, Kang TE, Lee C, Kang H, Shin M, Wang C, Ma B, Jeong U, Kim T-S. et al. Flexible, highly efficient all-polymer solar cells. Nat Commun. 2015;6:8547

12. Onorato J, Pakhnyuk V, Luscombe CK. Structure and design of polymers for durable, stretchable organic electronics. Polym J. 2017;49:41–60.

13. Kang SD, Snyder GJ. Charge-transport model for conducting polymers. Nat Mater. 2017;16:252–7.

14. Chang J-F, Sirringhaus H, Giles M, Heeney M, McCulloch I. Relative importance of polaron activation and disorder on charge transport in high-mobility conjugated polymer field-effect transistors. Phys Rev B. 2007;76:205204

15. DeLongchamp DM, Kline RJ, Lin EK, Fischer DA, Richter LJ, Lucas LA, Heeney M, McCulloch I, Northrup JE. High carrier mobility polythiophene thin films: structure determination by experiment and theory. Adv Mater. 2007;19:833–7.

16. Misra M, Andrienko D, Baumeier B, Faulon J-L, von Lilienfeld OA. Toward quantitative structure–property relationships for charge transfer rates of polycyclic aromatic hydrocarbons. J Chem Theory Comput. 2011;7:2549–55.

17. Gao D, Chen Z, Huang J, Zhang W, Wei C, Lin Z, Li D, Yu G. Microstructure engineering of polymer semiconductor thin films for high-performance field-effect transistors using a bi-component processing solution. J Mater Chem C. 2017;5:3568–78.

18. Ye L, Xiong Y, Li S, Ghasemi M, Balar N, Turner J, Gadisa A, Hou J, O'Connor BT, Ade H. Precise manipulation of multi-length scale morphology and its influence on eco-friendly printed all-polymer solar cells. Adv Funct Mater. 2017;27:1702016

19. Ma W, Yang G, Jiang K, Carpenter JH, Wu Y, Meng X, McAfee T, Zhao J, Zhu C, Wang C. et al. Influence of processing parameters and molecular weight on the morphology and properties of high-performance PffBT4T-2OD:PC $_{71}$ BM organic solar cells. Adv Energy Mater. 2015;5:1501400

20. Liu Y, Zhao J, Li Z, Mu C, Ma W, Hu H, Jiang K, Lin H, Ade H, Yan H. Aggregation and morphology control enables multiple cases of high-efficiency polymer solar cells. Nat Commun. 2014;5:5293

21. Diao Y, Shaw L, Bao Z, Mannsfeld SCB. Morphology control strategies for solution-processed organic semiconductor thin films. Energy Environ Sci. 2014;7:2145–59.

22. Botiz I, Stingelin N. Influence of molecular conformations and microstructure on the optoelectronic properties of conjugated polymers. Materials (Basel). 2014;7:2273–300.

23. Mazzio KA, Rice AH, Durban MM, Luscombe CK. Effect of regioregularity on charge transport and structural and excitonic coherence in poly(3-hexylthiophene) nanowires. J Phys Chem C. 2015;119:14911–8.

24. Spano FC, Silva C. H- and J-aggregate behavior in polymeric semiconductors. Annu Rev Phys Chem. 2014;65:477–500.

25. Chang M, Su Z, Egap E. Alignment and charge transport of one-dimensional conjugated polymer nanowires in insulating polymer blends. Macromolecules. 2016;49:9449–56.

26. Lu G, Chen J, Xu W, Li S, Yang X. Aligned polythiophene and its blend film by direct-writing for anisotropic charge transport. Adv Funct Mater. 2014;24:4959–68.

27. Rojo MM, Martín J, Grauby S, Borca-Tasciuc T, Dilhaire S, Martin-Gonzalez M. Decrease in thermal conductivity in polymeric P3HT nanowires by size-reduction induced by crystal orientation: new approaches towards thermal transport engineering of organic materials. Nanoscale. 2014;6:7858–65.

28. Lim JA, Liu F, Ferdous S, Muthukumar M, Briseno AL. Polymer semiconductor crystals. Mater Today. 2010;13:14–24.

29. Kim DH, Park YD, Jang Y, Kim S, Cho K. Solvent vapor-induced nanowire formation in poly(3-hexylthiophene) thin films. Macromol Rapid Commun. 2005;26:834–9.

30. Zhu Z, Wang J, Wei B. Self-assembly of ordered poly(3-hexylthiophene) nanowires for organic field-effect transistor applications. Physica E Low Dimens Syst Nanostruct. 2014;59:83–7.

31. Mun S, Park Y, Lee Y-EK, Sung MM. Highly sensitive ammonia gas sensor based on single-crystal poly(3-hexylthiophene) (P3HT) organic field effect transistor. Langmuir. 2017;33:13554–60.

32. Briseno AL, Mannsfeld SCB, Jenekhe SA, Bao Z, Xia Y. Introducing organic nanowire transistors. Mater Today. 2008;11:38–47.

33. Kim FS, Ren G, Jenekhe SA. One-dimensional nanostructures of π-conjugated molecular systems: assembly, properties, and applications from photovoltaics, sensors, and nanophotonics to nanoelectronics. Chem Mater. 2011;23:682–732.

34. Lindner SM, Thelakkat M. Nanostructures of N-type organic semiconductor in a P-type matrix via self-assembly of block copolymers. Macromolecules. 2004;37:8832–5.

35. Wicklein A, Ghosh S, Sommer M, Würthner F, Thelakkat M. Self-assembly of semiconductor organogelator nanowires for photoinduced charge separation. ACS Nano. 2009;3:1107–14.

36. Ford MJ, Wang M, Patel SN, Phan H, Segalman RA, Nguyen T-Q, Bazan GC. High mobility organic field-effect transistors from majority insulator blends. Chem Mater. 2016;28:1256–60.

37. Schenning APHJ, Meijer EW. Supramolecular electronics; nanowires from self-assembled pi-conjugated systems. Chem Commun (Camb). 2005;26:3245–58.

38. Ihn KJ, Moulton J, Smith P. Whiskers of poly(3-Alkylthiophene)s. J Polym Sci Part B Polym Phys. 1993;31:735–42.

39. Mårdalen J, Samuelsen EJ, Pedersen AØ. The nucleation process and the crystalline structure of poly(3-alkylthiophenes) precipitated from marginal solvents. Synth Met. 1993;55:378–83.

40. Liu J, Arif M, Zou J, Khondaker SI, Zhai L. Controlling poly (3-hexylthiophene) crystal dimension: nanowhiskers and nanoribbons. Macromolecules. 2009;42:9390–3.

41. Kleinhenz N, Rosu C, Chatterjee S, Chang M, Nayani K, Xue Z, Kim E, Middlebrooks J, Russo PS, Park JO. et al. Liquid crystalline poly(3-hexylthiophene) solutions revisited: role of time-dependent self-assembly. Chem Mater. 2015;27:2687–94.

42. Chang M, Lee J, Chu P-H, Choi D, Park B, Reichmanis E. Anisotropic assembly of conjugated polymer nanocrystallites for enhanced charge transport. ACS Appl Mater Interfaces. 2014;6:21541–9.

43. Chang M, Lee J, Kleinhenz N, Fu B, Reichmanis E. Photoinduced anisotropic supramolecular assembly and enhanced charge transport of poly(3-hexylthiophene) thin films. Adv Funct Mater. 2014;24:4457–65.

44. Chu P-H, Kleinhenz N, Persson N, McBride M, Hernandez JL, Fu B, Zhang G, Reichmanis E. Toward precision control of nanofiber orientation in conjugated polymer thin films: impact on charge transport. Chem Mater. 2016;28:9099–109.

45. Aiyar AR, Hong J-I, Izumi J, Choi D, Kleinhenz N, Reichmanis E. Ultrasound-induced ordering in poly(3-hexylthiophene): role of molecular and process parameters on morphology and charge transport. ACS Appl Mater Interfaces. 2013;5:2368–77.

46. Kim B-G, Kim M-S, Kim J. Ultrasonic-assisted nanodimensional self-assembly of poly-3-hexylthiophene for organic photovoltaic cells. ACS Nano. 2010;4:2160–6.

47. Choi D, Chang M, Reichmanis E. Controlled assembly of poly (3-hexylthiophene): managing the disorder to order transition on the nano- through meso-scales. Adv Funct Mater. 2015;25:920–7.

48. Persson NE, Rafshoon J, Naghshpour K, Fast T, Chu P-H, McBride M, Risteen B, Grover M, Reichmanis E. High-throughput image analysis of fibrillar materials: a case study on polymer nanofiber packing, alignment, and defects in organic field effect transistors. ACS Appl Mater Interfaces. 2017;9:36090–102.

49. Persson NE, Chu P-H, McBride M, Grover M, Reichmanis E. Nucleation, growth, and alignment of poly(3-hexylthiophene) nanofibers for high-performance OFETs. Acc Chem Res. 2017;50:932–42.

50. Wang G, Persson N, Chu P-H, Kleinhenz N, Fu B, Chang M, Deb N, Mao Y, Wang H, Grover MA. et al. Microfluidic crystal engineering of π-conjugated polymers. ACS Nano. 2015;9:8220–30.

51. Li J-H, Xi Y, Pozzo LD, Xu J-T, Luscombe CK. Macroscopically aligned nanowire arrays of p-conjugated polymers via shear-enhanced crystallization. J Mater Chem C. 2017;5128:5128–34.

52. Xi Y, Pozzo LD. Electric field directed formation of aligned conjugated polymer fibers. Soft Matter. 2017;13:3894–908.

53. Diao Y, Tee BC-K, Giri G, Xu J, Kim DH, Becerril HA, Stoltenberg RM, Lee TH, Xue G, Mannsfeld SCB, et al. Solution coating of large-area organic semiconductor thin films with aligned single-crystalline domains. Nat Mater. 2013;12:665–71.

54. Bucella SG, Luzio A, Gann E, Thomsen L, McNeill CR, Pace G, Perinot A, Chen Z, Facchetti A, Caironi M. Macroscopic and high-throughput printing of aligned nanostructured polymer semiconductors for MHz large-area electronics. Nat Commun. 2015;6:8394

55. Wang G, Chu P-H, Fu B, He Z, Kleinhenz N, Yuan Z, Mao Y, Wang H, Reichmanis E. Conjugated polymer alignment: synergisms derived from microfluidic shear design and UV irradiation. ACS Appl Mater Interfaces. 2016;8:24761–72.

56. Lu Guanghao, Tang Haowei, Qu Yunpeng, Ligui Li A, Yang X. Enhanced electrical conductivity of highly crystalline polythiophene/insulating-polymer composite. Macromolecules. 2007;40:6579–84.

57. Lim JA, Kim J-H, Qiu L, Lee WH, Lee HS, Kwak D, Cho K. Inkjet-printed single-droplet organic transistors based on semiconductor nanowires embedded in insulating polymers. Adv Funct Mater. 2010;20:3292–7.

58. Qiu L, Lee WH, Wang X, Kim JS, Lim JA, Kwak D, Lee S, Cho K. Organic thin-film transistors based on polythiophene nanowires embedded in insulating polymer. Adv Mater. 2009;21:1349–53.

59. Chang M, Choi D, Wang G, Kleinhenz N, Persson N, Park B, Reichmanis E. Photoinduced anisotropic assembly of conjugated polymers in insulating polymer blends. ACS Appl Mater Interfaces. 2015;7:14095–103.

60. Liu X, Long Y-Z, Liao L, Duan X, Fan Z. Large-scale integration of semiconductor nanowires for high-performance flexible electronics. ACS Nano. 2012;6:1888–900.

61. Choi D, Kim H, Persson N, Chu P-H, Chang M, Kang J-H, Graham S, Reichmanis E. Elastomer–polymer semiconductor blends for high-performance stretchable charge transport networks. Chem Mater. 2016;28:1196–204.

62. Kim FS, Jenekhe SA. Charge transport in poly(3-butylthiophene) nanowires and their nanocomposites with an insulating polymer. Macromolecules. 2012;45:7514–9.

63. Xu J, Wang S, Wang G-JN, Zhu C, Luo S, Jin L, Gu X, Chen S, Feig VR, To JWF. et al. Highly stretchable polymer semiconductor films through the nanoconfinement effect. Science. 2017;355:59–64.

64. Ji Y, Xiao C, Heintges GHL, Wu Y, Janssen RAJ, Zhang D, Hu W, Wang Z, Li W. Conjugated polymer with ternary electron-deficient units for ambipolar nanowire field-effect transistors. J Polym Sci Part A Polym Chem. 2016;54:34–8.

65. Xiao C, Zhao G, Zhang A, Jiang W, Janssen RAJ, Li W, Hu W, Wang Z. High performance polymer nanowire field-effect transistors with distinct molecular orientations. Adv Mater. 2015;27:4963–8.

66. Lezzi F, Ferrari G, Pennetta C, Pisignano D. Suppression of low-frequency electronic noise in polymer nanowire field-effect transistors. Nano Lett. 2015;15:7245–52.

67. Jeong JW, Lee YD, Kim YM, Park YW, Choi JH, Park TH, Soo CD, Won SM, Han IK, Ju BK. The response characteristics of a gas sensor based on poly-3-hexylithiophene thin-film transistors. Sens Actuators B Chem. 2010;146:40–5.

68. Mohammad F. Compensation behaviour of electrically conductive polythiophene and polypyrrole. J Phys D Appl Phys. 1998;31:951–9.

69. Fukuda H, Yamagishi Y, Ise M, Takano N. Gas sensing properties of poly-3-hexylthiophene thin film transistors. Sens Actuators B Chem. 2005;108:414–7.

70. Jia Y, Zuo X, Lou X, Miao M, Cheng Y, Min X, Li X, Xia F. Rational designed bipolar, conjugated polymer-DNA composite beacon for the sensitive detection of proteins and ions. Anal Chem. 2015;87:3890–4.

71. Chiang C-H, Pangeni D, Nesterov EE. Higher energy gap control of fluorescence in conjugated polymers: turn-on amplifying chemosensor for hydrogen sulfide. Macromolecules. 2017;50:6961–6.

72. Gicevicius M, Ramanaviciene A, Mikoliunaite L, Ramanavicius A. Optical sensors based on electrochromic conducting polymers. In 2017 IEEE 7th international conference Nanomaterials: application & properties (NAP). Odessa: IEEE; 2017. p. 04NB29-1–04NB29-3.

73. Chu F, Tsiminis G, Spooner NA, Monro TM. Explosives detection by fluorescence quenching of conjugated polymers in suspended core optical fibers. Sens Actuators B Chem. 2014;199:22–26.

74. He F, Tang Y, Wang S, Li Y, Zhu D. Fluorescent amplifying recognition for DNA G-quadruplex folding with a cationic conjugated polymer: a platform for homogeneous potassium detection. J Am Chem Soc. 2005;127:12343–6.

75. Liu X, Tang Y, Wang L, Zhang J, Song S, Fan C, Wang S. Optical detection of mercury(II) in aqueous solutions by using conjugated polymers and label-free oligonucleotides. Adv Mater. 2007;19:1471–4.

76. Ho H-A, Béra-Abérem M, Leclerc M. Optical sensors based on hybrid DNA/conjugated polymer complexes. Chemistry. 2005;11:1718–24.

77. McQuade DT, Pullen AE, Swager TM. Conjugated polymer-based chemical sensors. Chem Rev. 2000;100:2537–74.

78. Zhang C, Wang Y, Cheng S, Zhang X, Fu B, Hu W. Assembly of π-conjugated nanosystems for electronic sensing devices. Adv Electron Mater. 2017;3:1700209

79. García M, Batalla P, Escarpa A. Metallic and polymeric nanowires for electrochemical sensing and biosensing. TrAC Trends Anal Chem. 2014;57:6–22.

80. Knopfmacher O, Hammock ML, Appleton AL, Schwartz G, Mei J, Lei T, Pei J, Bao Z. Highly stable organic polymer field-effect transistor sensor for selective detection in the marine environment. Nat Commun. 2014;5:2954

81. O'Brien GA, Quinn AJ, Tanner DA, Redmond G. A single polymer nanowire photodetector. Adv Mater. 2006;18:2379–83.

82. Wakayama Y, Hayakawa R, Seo H-S. Recent progress in photoactive organic field-effect transistors. Sci Technol Adv Mater. 2014;15:24202

83. Gu P, Yao Y, Feng L, Niu S, Dong H. Recent advances in polymer phototransistors. Polym Chem. 2015;6:7933–44.

84. Liu Y, Wang H, Dong H, Jiang L, Hu W, Zhan X. High performance photoswitches based on flexible and amorphous D-A polymer nanowires. Small. 2013;9:294–9.

85. Liu Y, Dong H, Jiang S, Zhao G, Shi Q, Tan J, Jiang L, Hu W, Zhan X. High performance nanocrystals of a donor–acceptor conjugated polymer. Chem Mater. 2013;25:2649–55.

86. Lei Y, Li N, Chan W-KE, Ong BS, Zhu F. Highly sensitive near infrared organic phototransistors based on conjugated polymer nanowire networks. Org Electron. 2017;48:12–8.

87. Zhu M, Lv S, Wang Q, Zhang G, Lu H, Qiu L. Enhanced near-infrared photoresponse of organic phototransistors based on single-component donor–acceptor conjugated polymer nanowires. Nanoscale. 2016;8:7738–48.

88. Terra IAA, Sanfelice RC, Valente GT, Correa DS. Optical sensor based on fluorescent PMMA/PFO electrospun nanofibers for monitoring volatile organic compounds. J Appl Polym Sci. 2018;135:46128

89. Wang X, Kim Y-G, Drew C, Ku B-C, Kumar J, Samuelson LA. Electrostatic assembly of conjugated polymer thin layers on electrospun nanofibrous membranes for biosensors. Nano Lett. 2004;4:331–4.

90. Wang X, Drew C, Lee S-H, Senecal KJ, Kumar J, Samuelson LA. Electrospun nanofibrous membranes for highly sensitive optical sensors. Nano Lett. 2002;2:1273–5.

91. An B-K, Gihm SH, Chung JW, Park CR, Kwon S-K, Park SY. Color-tuned highly fluorescent organic nanowires/nanofabrics: easy massive fabrication and molecular structural origin. J Am Chem Soc. 2009;131:3950–7.

92. Di Benedetto F, Camposeo A, Pagliara S, Mele E, Persano L, Stabile R, Cingolani R, Pisignano D. Patterning of light-emitting conjugated polymer nanofibres. Nat Nanotechnol. 2008;3:614–9.

93. Luo J, Lei T, Wang L, Ma Y, Cao Y, Wang J, Pei J. Highly fluorescent rigid supramolecular polymeric nanowires constructed through multiple hydrogen bonds. J Am Chem Soc. 2009;131:2076–7.

94. O'Carroll D, Lieberwirth I, Redmond G. Microcavity effects and optically pumped lasing in single conjugated polymer nanowires. Nat Nanotechnol. 2007;2:180–4.

95. Chen G, Xu W, Zhu D. Recent advances in organic polymer thermoelectric composites. J Mater Chem C. 2017;5:4350–60.

96. Bharti M, Singh A, Samanta S, Aswal DK. Conductive polymers for thermoelectric power generation. Prog Mater Sci. 2018;93:270–310.

97. Yao H, Fan Z, Cheng H, Guan X, Wang C, Sun K, Ouyang J. Recent development of thermoelectric polymers and composites. Macromol Rapid Commun. 2018;39:1700727

98. Chen Y, Zhao Y, Liang Z. Solution processed organic thermoelectrics: towards flexible thermoelectric modules. Energy Environ Sci. 2015;8:401–22.

99. Chabinyc M. Behind organics' thermopower. Nat Mater. 2014;13:119–21.

100. Patel SN, Glaudell AM, Kiefer D, Chabinyc ML. Increasing the thermoelectric power factor of a semiconducting polymer by doping from the vapor phase. ACS Macro Lett. 2016;5:268–72.

101. Patel SN, Glaudell AM, Peterson KA, Thomas EM, O'Hara KA, Lim E, Chabinyc ML. Morphology controls the thermoelectric power factor of a doped semiconducting polymer. Sci Adv. 2017;3:e1700434

102. Hiura S, Okada N, Wakui J, Narita H, Kanehashi S, Shimomura T. Thermoelectric properties of poly(3-hexylthiophene) nanofiber mat with a large void fraction. Materials (Basel). 2017;10:468

103. Giridharagopal R, Flagg LQ, Harrison JS, Ziffer ME, Onorato J, Luscombe CK, Ginger DS. Electrochemical strain microscopy probes morphology-induced variations in ion uptake and performance in organic electrochemical transistors. Nat Mater. 2017;16:737–42.

104. Zhang J, Zhang K, Xu F, Wang S, Qiu Y. Thermoelectric transport in ultrathin poly(3,4-ethylenedioxythiophene) nanowire assembly. Compos Part B Eng. 2018;136:234–40.